JOURNAL OF AGRICULTURAL AND FOOD CHEMISTRY

Article

pubs.acs.org/JAFC

Faster Fermentation of Cooked Carrot Cell Clusters Compared to Cell Wall Fragments *in Vitro* by Porcine Feces

Li Day,*[,†] Justine Gomez,[†] Sofia K. Øiseth,[†] Michael J. Gidley,[‡] and Barbara A. Williams[‡]

[†]CSIRO Food and Nutritional Sciences, 671 Sneydes Road, Werribee, Victoria 3030, Australia

[‡]ARC Centre of Excellence in Plant Cell Walls, Centre for Nutrition and Food Sciences, The University of Queensland, St Lucia, Brisbane, Queensland 4072, Australia

ABSTRACT: Plant cell walls are the major structural component of fruits and vegetables, which break down to cell wall particles during ingestion (oral mastication) or food processing. The major health-promoting effect of cell walls occurs when they reach the colon and are fermented by the gut microbiota. In this study, the fermentation kinetics of carrot cell wall particle dispersions with different particle size and microstructure were investigated *in vitro* using porcine feces. The cumulative gas production and short-chain fatty acids (SCFAs) produced were measured at time intervals up to 48 h. The results show that larger cell clusters with an average particle size ($d_{0.5}$) of 298 and 137 μm were more rapidly fermented and produced more SCFAs and gas than smaller single cells (75 μm) or cell fragments (50 μm), particularly between 8 and 20 h. Confocal microscopy suggests that the junctions between cells provides an environment that promotes bacterial growth, outweighing the greater specific surface area of smaller particles as a driver for more rapid fermentation. The study demonstrates that it may be possible, by controlling the size of cell wall particles, to design plant-based foods for fiber delivery and promotion of colon fermentation to maximize the potential for human health.

KEYWORDS: *Plant cell wall, particle size, cumulative gas production, short-chain fatty acids (SCFAs)*

INTRODUCTION

It is well-accepted that regular consumption of fruits and vegetables can provide positive health benefits to consumers, such as reducing the risk of cardiovascular diseases, colorectal cancer, type 2 diabetes, and obesity.[1−4] This impact is derived from a combination of the physical and physiological functionality of cell wall materials and a range of health beneficial micronutrients, including vitamins, minerals, polyphenols, carotenoids, etc. Plant cell walls are the major structural component of fruits and vegetables, consisting primarily of cellulose, hemicellulose, and pectin, which form a scaffold matrix with an intertwined connected structure. Plant tissue foods are broken down to small particles during food processing and/or after oral mastication. Because there are no mammalian enzymes within the stomach or small intestine that are capable of hydrolyzing the main components of plant cell walls, they pass along the gastrointestinal tract without being digested, absorbed, or metabolized, until they reach the terminal ileum and colon, where they may be used as fermentation substrates by the gut microbial community.[5,6]

The continued emphasis on the importance of fruit and vegetable intake in the Western diet, in conjunction with consumer demand for natural ingredients in manufactured food products, has led to a significant increase in the use of plant cellular materials as functional food ingredients, in particular from the byproduct of industrial fruit and vegetable processing.[7,8] Our recent work has shown that the size and morphology of cell wall particles are important in determining their rheological properties,[9,10] their interaction with other food ingredients,[11] their ability to structure foods,[12] and the bioavailability of carotenoids.[13] The ability of plant cell and cell wall structures to hold water and provide high viscosity at a relatively low particle concentration can provide positive physiological benefits, such as slowing the gastric emptying rate and reducing the gastrointestinal transit time, as shown for individual polysaccharides.[14,15] Some cell walls or constituent polysaccharides may also bind bile acids and impede micelle formation, thus increasing fecal excretion of bile acids and cholesterol or influencing the absorption of nutrients.[16] However, the major health-promoting effect of cell walls occurs when they reach the colon and are fermented by the gut microbiota.

Dietary polysaccharides that reach the human large intestine have a major impact on gut microbial ecology and health.[17] This is partly due to their ability to increase the activity and growth of some health-promoting bacteria (prebiotic effect) by providing an energy source (selective substrate), which can thus alter the gut bacterial community composition.[3,18,19] Fermentation in the large intestine also leads to the production of short-chain fatty acids (SCFAs), gas (hydrogen, carbon dioxide, and methane), and other metabolites (ammonia, phenols, etc.). The primary SCFAs generated by fermentation are acetate, propionate, and butyrate, accounting for 83−95% of the total SCFA concentration in the large intestine.[20] Butyrate is absorbed by the colonic mucosa, used as its major energy source, and plays a key role in the health of the colon.[21,22] It affects both the stimulation of cell division and the regulation of apoptosis and has been shown to increase apoptosis in human colonic tumor cell lines.[23,24] The SCFAs absorbed into the portal blood

Received: December 4, 2011
Revised: February 27, 2012
Accepted: March 5, 2012
Published: March 5, 2012

Table 1. Particle Sizes of Carrot Cell Wall Dispersions Obtained with Different Heating and Blending Conditions

	heating		blending				
sample code[a]	temperature (°C)	time (min)	setting	time (min)	principal particle morphology	particle size, $d_{0.5}$ (μm)	total solids (%)
CWP1	80	30	1	2	large cell clusters	298	2.7
CWP2	80	30	1	8	small cell clusters	137	3.2
CWP3	100	30	1	8	single cells	75	2.8
CWP4	100	40	5	8	cell fragments	50	3.4

[a]CWP = cell wall particle dispersion.

system can further influence lipid metabolism.[22] Moreover, the accumulation of SCFAs lowers the colonic pH counterbalancing potentially toxic ammonia (NH_3). Ammonia can also be taken up by bacteria as a source of nitrogen for growth, reducing the amounts of NH_3 absorbed into the bloodstream. The bacteria are then excreted in the feces rather than the ammonia being lost to the environment as urea from the urine.[25]

Most research into the understanding of the physiological impact of dietary fiber has been on purified polysaccharides, particularly from cereal sources, including resistant starch.[22,26,27] It has been demonstrated that the nature and chemical structure of individual polysaccharides and the matrix structure and physical properties of the fiber can significantly affect how materials are fermented.[15,28−31] However, the detailed interactions between fiber and bacteria are still not well-understood. In particular, the reason why some fibers are fermented more rapidly and to a greater extent than others and lead to the production of a different ratio of end products has not been completely elucidated. Although the carbohydrate composition affects fiber fermentation, it is likely that the first limiting parameter is the accessibility of bacteria to the fiber (cell wall) matrix. It is generally assumed that most bacteria must have physical access and adhere to fiber materials to begin the digestion process, even if some bacteria can release extracellular enzymes within close proximity to the wall and achieve its degradation.[15] Soluble polysaccharides are generally more rapidly fermented than equivalent polysaccharides included in an organized network, such as cellulose-based composites.[31]

For plant cellular structures and cell walls, a combination of the particle size and architecture determines the surface area available to bacteria and may therefore control, at least partially, the fermentability of the cell wall particles. For cereal-derived particles, comparative studies of different cereal types[30] and coarse versus fine milling of wheat bran fractions[29] using *in vitro* fermentation suggests that smaller particles are fermented more rapidly. However, there is no comparable data for fruit or vegetable fermentation as a function of the particle size. We hypothesized that reducing the particle size (and potentially increasing cell wall porosity) by a combination of heat and shear would lead to faster bacterial fermentation. This study was therefore designed to investigate the fermentation kinetics and the end-product profiles of cooked carrot cell wall particles with different particle size and structural morphology using an *in vitro* cumulative gas production technique with a porcine fecal inoculum. Pigs are often used as a model for human gastrointestinal parameters, because their tract is most similar to that of humans compared to other domestic animals and because they are omnivorous. The cumulative gas production and the end products, including SCFAs and ammonia, were monitored at time intervals up to 48 h, to determine both the profile and extent of *in vitro* fermentation. A greater understanding of the relationships between the fermentation rate and plant cellular structure would provide added information for the development and increased use of fruit- and vegetable-based cell wall materials in foods for the optimization of colonic health.

MATERIALS AND METHODS

Plant Cell Wall Particle Dispersions. Fresh carrots were purchased from a local supermarket. Carrots were peeled and cut into approximately 2 cm pieces. Water (200 g) was preheated to either 80 or 100 °C depending upon the processing regime, to obtain required cell wall particle sizes and morphology.[9] Carrot pieces (200 g) were then added to the water, heated for 30 or 40 min at the required temperature, and cooled immediately in an ice bath. After cooling, an additional amount of water was added to make up for the evaporated volume. This mixture was then transferred to a kitchen blender (Café Series model PB9500, Sunbeam Australia) and homogenized for an appropriate time at the required speed set (Table 1). Four carrot dispersions were obtained with various particle sizes and morphology, i.e., predominantly cell clusters, single cells, or cell wall fragments.

Soluble matter was removed by centrifuging the dispersions at 11600*g* for 15 min at 24 °C (RC-5C centrifuge, GSA Rotor, Sorvall Instruments) and filtering through Whatman No. 1 filter paper. The remaining pellet was collected and washed with Milli-Q water until the refractive index of the filtrate was below 0.2° Brix.

Total Solids. The total solids content of the dispersions was measured by drying to a constant weight at 103 °C according to the ISO method 6496.

Particle Size Distribution. The apparent particle size distribution of the dispersions was measured by laser light scattering using a Malvern Mastersizer 2000 instrument (Malvern Instruments, Ltd., Worcestershire, U.K.). Deionized water was used as the dispersant. A differential refractive index of 1.173 (1.560 for particle/1.330 for deionized water) and absorption of 0.1 were used as the optical properties of the dispension. The particle calculation was set for irregular particles, and each dispersion was measured in duplicate. The volume median diameter value $d_{0.5}$ (the size at which 50% of the particles are smaller and 50% are larger) was used as the average particle size of the dispersion.

Confocal Laser Scanning Microscopy (CLSM). The morphologies of the plant cell wall particles were observed using a Leica TCS SP5 confocal laser scanning microscope (Leica Microsystems, Wetzlar, Germany). Samples were diluted 2−4 times with water to separate the plant fragments and then stained with the fluorescent dye Congo Red (0.005%) prior to observation under a HC PL APO 20× or a HCX PL APO 63× objective at room temperature. The fluorescent dye was excited by an argon 488 nm laser, and the emitted light was collected at 544−663 nm.

To observe the bacteria attached to the cell wall particles, a Live/Dead *Bac*Light Bacterial Viability Kit (Molecular Probes, Inc.) with a mixture of SYTO 9 (green-fluorescent nucleic acid stain) and propidium iodide (red-fluorescent nucleic acid stain) was used. The fluorescent dyes were excited by an argon 488 nm laser, and emitted light was collected at 500−525 nm (live cells) and 650−725 nm (dead cells).

CLSM images of fermented carrot samples were analyzed by AnalySIS (Olympus Soft Imaging Solutions Pte, Ltd.). Particles at least 100 pixels in size were included, and the image analysis data were further processed by statistical analysis software, Minitab14 (Minitab, Inc., State College, PA).

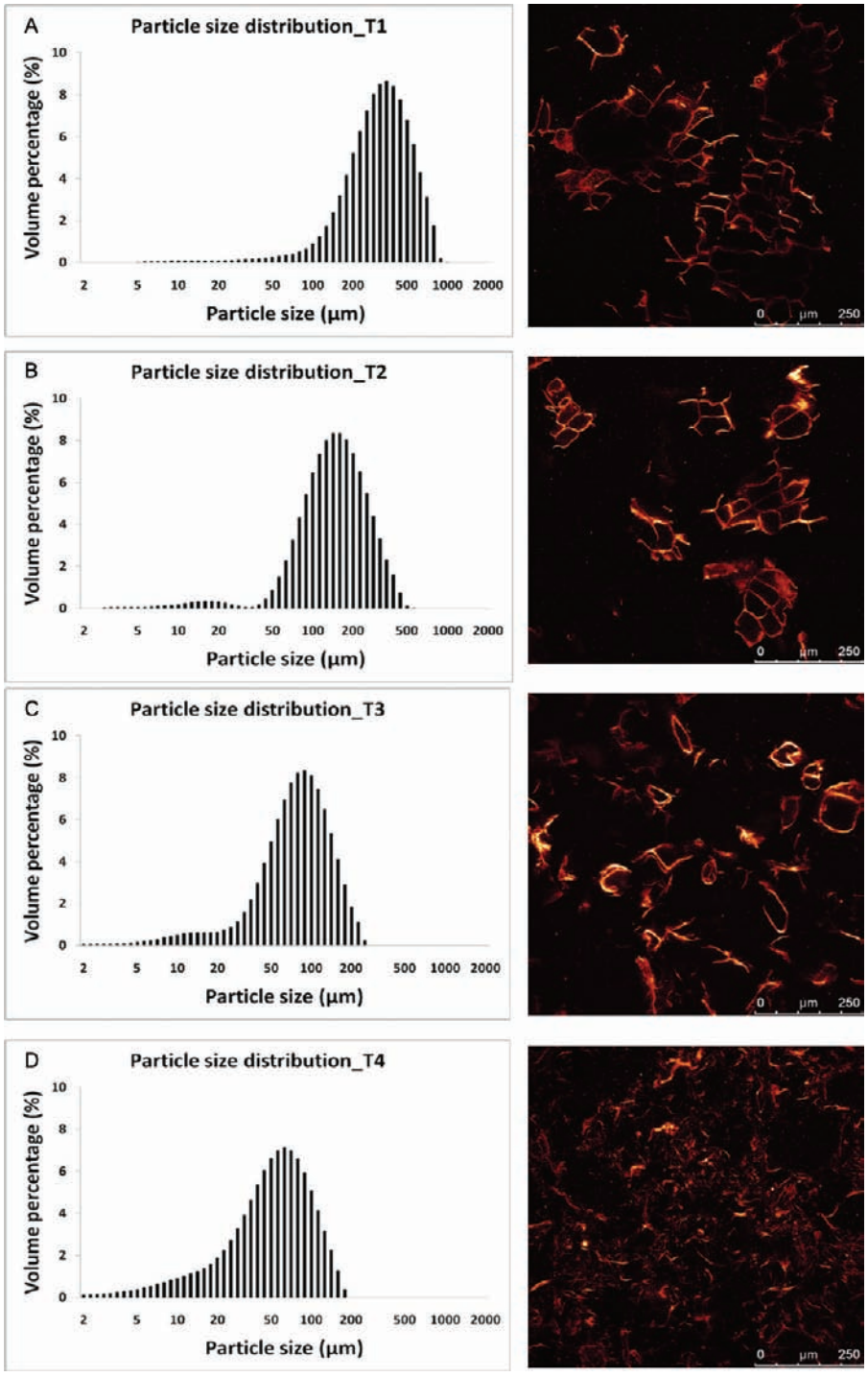

Figure 1. Particle size distribution and corresponding confocal images of carrot cell wall particle dispersions used for *in vitro* fermentation.

Preparation of Substrates. Half of the dispersions were subjected to a simple washing pretreatment at acidic and neutral pH values, designed to remove soluble components, e.g., sugars, amino acids, etc., which would be expected to be absorbed prior to reaching the colon. This was carried out by adjusting the pH of the dispersion to 2 by the addition of 1 M HCl, followed by incubation in a water bath at 37 °C for 20 min with constant shaking. The pH of the dispersion was then readjusted to pH 7 using 1 M $NaHCO_3$ and incubated in the shaking water bath at 37 °C for a further 20 min. Digestive enzymes, such as amylase, protease, and lipase, were not used because there are only minor amounts of their substrates in carrots.

The resulting substrates were called CWP1-W−CWP4-W, with W referring to the samples having gone through the washing pretreatment. The other half of the dispersions were used directly as substrates for *in vitro* fermentation without the washing pretreatment *in vitro* digestion step and were called CWP1-NW−CWP4-NW.

Collection and Preparation of Inoculum. The porcine inoculum was prepared as described previously.[32] In brief, feces were collected from five pigs between 50 and 60 kg. For 10 days previously, the pigs were fed a standard semi-defined diet based on readily digestible maize starch and fishmeal. This is the standard procedure for this method. The diet was designed to be as free as possible of fermentable carbohydrates to avoid adaptation of elements of the microbial population to that substrate. Feces were collected

rectally and placed into a warmed vacuum flask filled with CO_2. The feces from all animals were combined and diluted 1:5 with prewarmed, sterile saline (0.9% NaCl). This was then mixed for 60 s using a hand-held blender and filtered through four layers of muslin cloth. This mixing step was to ensure that the resulting inoculum contained both non-adhering and adhering microorganisms. All procedures were carried out under a constant stream of CO_2.

The anaerobic medium was prepared according to the method described by Williams et al.[33] to contain several forms of nitrogen and most of the known micronutrients that anaerobic culturable bacterial species require for growth.

Measurement of Cumulative Gas Production. The *in vitro* cumulative gas production technique was carried out according to the method by Williams et al.[33] Briefly, the substrate (3 g in fresh weight equivalent to approximately 0.1 g of dry material) was added to each 60 mL serum bottle, with 38 mL of total medium, and kept at 4 °C overnight. The bottles were prewarmed to 39 °C for ∼5 h prior to inoculation, at which time 2 mL of inoculum was added per serum bottle, within 2 h of collection of the feces. A total of 20 gas readings were taken at regular intervals over 48 h (0, 1, 2, 4, 6, 8, 10, 12, 15, 18, 21, 24, 27, 30, 33, 36, 39, 42, and 48 h). Four replicates of each substrate were fermented for the entire 48 h. At the end of the fermentation time, all bottles were plunged into iced water and frozen to inhibit any further fermentation.

Three different blanks (i.e., no substrate) were used. There was one blank without inoculum (BL − I0) and two others with inoculum. One blank with inoculum remained in the incubator for the duration of fermentation (BL + I48), while the other was inoculated and then autoclaved immediately to give a starting value (BL + I0).

Profiles of cumulative gas production corrected as milliliters of gas produced per gram of dry matter over time were fitted to the monophasic model described by Groot et al.[34] The dry matter cumulative volume (DMCV) (total gas produced) was calculated as

$$\mathrm{DMCV} = \frac{A}{1 + (C/t)^B} \tag{1}$$

where A is the asymptotic gas production (DMCV_∞), B is the switching characteristic of the curve, C is the time at which half of the asymptote has been reached ($t_{1/2}$), and t is the fermentation time (in hours). The maximum rate of gas production (R_{max}) and the time at which it occurs (TR_{max}), were calculated as[35]

$$TR_{\max} = C(((B-1)/(B+1))^{(1/B)}) \tag{2}$$

$$R_{\max} = (A(C^B)B(TR_{\max}{}^{(-B-1)}))/(1 + (C^B)TR_{\max}{}^{(-B)})^2 \tag{3}$$

Post-fermentation Analyses. A total of 16 extra bottles per substrate were simultaneously inoculated with the bottles for gas production measurements (2 replicates per 8 time intervals). These were then fermented and removed at the following fixed times during the fermentation: 0, 2, 6, 8, 12, 18, 24, 30, and 36 h. The gas production bottles (four replicates) were stopped at 48 h. These fermentations were also stopped by putting the bottles into ice slurry for 30 min. The contents of all bottles were centrifuged at 3000*g* for 15 min at 4 °C. The solids were collected for CLSM microscopic observation. The pH of the supernatants was recorded. The SCFAs in supernatants were analyzed by gas chromatography using a polar capillary column DB-FFAP, with high-purity helium at 35 kPa and 200 °C as the carrier gas and isocaproic acid as the internal standard. SCFAs are reported as millimoles per gram of dry matter weighed into the bottles. The SCFAs analyzed were acetate, propionate, butyrate, isobutyrate, valerate, and isovalerate.

The SCFA data were used to calculate the branched-chain ratio (BCR). The BCR is the ratio of the mainly branched-chain acids (branched-chain and valeric acids) to the straight-chain acids.[36] The former (including valeric acid) is associated with the metabolism of amino acids, while the latter comes from the breakdown of carbohydrates. Therefore, BCR is used here to indicate relative protein fermentation.

Ammonia was analyzed using a method modified from Baethgen and Alley[37] as described previously.[32] Briefly, ammonium nitrogen was determined colorimetrically, using the chemical reaction of ammonium ions $(NH_4)^+$ with sodium salicylate and nitroprusside in a weakly alkaline buffer, at a wavelength of 650 nm, using an ultraviolet/visible (UV/vis) spectrophotometer (automated discrete analyzer model AQ2+, SEAL Analytical, Ltd., Fareham, U.K.).

Statistical Analysis. Differences between substrates at each time interval were tested for significance using Tukey's studentized range test of multiple comparisons according to the following equation:

$$Y = \mu + S_i + \varepsilon_i \tag{4}$$

where Y is the result, μ is the mean, S_i is the effect of substrate i, and ε_i is the error term. The replicate effect was also tested but was not significant. Blank values were excluded from the analysis. Probability values of <0.05 were considered significant.

All statistical analyses were performed using the SAS NLIN (curve-fitting) and GLM (significant differences) procedures (Statistical Analysis Systems Institute 9.1, 2002/3).

RESULTS

Particle Size and Microstructure of Cell Wall Dispersions. Figure 1 shows the particle size distribution and microstructure of cell wall dispersions prepared with a combination of heating and homogenization. Heating up to 80 °C does not cause major loosening of pectin in the middle lamellae;[38] thus, further mechanical treatment broke up the plant tissues through random tearing across cell walls, resulting in cell wall clusters containing several intact cells and broken end cells (panels A and B of Figure 1). On the other hand, when a mechanical force was applied to the plant tissues heat-treated at 100 °C, cells separated primarily along cell junctions because of weakening of intercellular adhesion[9] to produce a particle dispersion mostly consisting of single cells with an average particle size of 75 μm (Figure 1C). More severe shear processing led to further breakdown of the tissues to irregular cell wall fragments with no distinctive cell structure (Figure 1D). The cell wall dispersions contained a heterogeneous distribution of different particles, although each of the dispersions could be characterized by the type of particle that was predominant in the distribution. The particle size and morphology of the dispersions were similar to those previously used for rheology and bioavailability studies.[9,10] The total solids contents of the dispersions were in the range of 2.7−3.4% (Table 1).

Pretreatment of Substrates for *in Vitro* Fermentation. Although neither digested nor absorbed in the stomach and small intestine, the cell and cell wall structure may be affected by the physicochemical environment prevailing in different sites of the digestive tract, particularly in relation to their soluble components. To reduce the soluble materials, which would normally be lost during passage through the stomach and small intestine, half of the cell wall dispersions were treated with a simple *in vitro* washing procedure prior to the *in vitro* fermentation. Particle size measurements and CLSM characterization showed that pretreatement of cell wall materials did not result in any change in the particle morphology (results not shown).

Cumulative Gas Production. Figure 2 shows typical gas accumulation profiles of the four cell wall particle dispersions for those that were not subjected to the washing procedure (Figure 2A) and those that were (Figure 2B). The gas production related to *in vitro* fermentation kinetics are summarized in Table 2. In comparison to the substrates, the blanks produced almost no gas and, therefore, are not shown. The gas

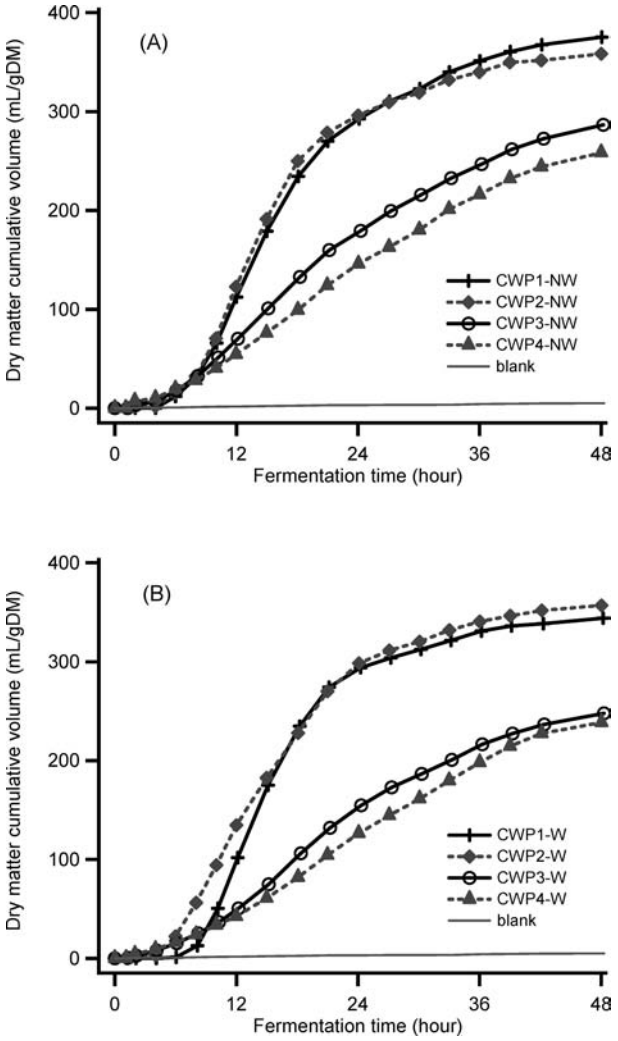

Figure 2. Representative cumulative gas profiles (mL/g of DM). (A) Cell wall particle dispersions that did not go through *in vitro* pH washing treatment. (B) Cell wall particle dispersions subjected to *in vitro* pH washing treatment prior to fermentation. CWP1, large cluster particles with an average particle size $d_{0.5}$ of 298 μm; CWP2, cluster particles with $d_{0.5}$ of 137 μm; CWP3, single cell particles with $d_{0.5}$ of 75 μm; and CWP4, cell fragment particles with $d_{0.5}$ of 50 μm.

production kinetics from the two cluster-cell substrates (CWP1 and CWP2) were similar. Likewise, the single-cell and cell-fragment substrates (CWP3 and CWP4) showed a similar pattern of gas production. However, there was a distinctive difference in the gas production kinetics between the large cluster-cell and small single-cell or cell-fragment substrates. A higher rate of gas production (R_{max}), in particular between 8 and 20 h of fermentation, was found for the large cluster-cell substrates (e.g., CWP1 and CWP2), indicating that they were fermented more rapidly than the small single-cell or cell-fragment substrates. However, it was noteworthy that fermentation rates up to 8 h were very similar for all substrates, suggesting that the presence of readily available carbohydrate was similar for all substrates.

There were significant differences in DMCV (total gas) produced after 48 h ($p < 0.0001$), the time at which half of the asymptote has been reached ($t_{1/2}$, $p < 0.0001$), the maximum rate of gas production (R_{max}, $p < 0.0001$), and the time at which the maximum rate of gas production occurred (TR_{max}, $p < 0.0001$) between the cluster-cell dispersions (CWP1 and CWP2) and the single-cell or cell-fragment dispersions (CWP3 and CWP4) but not between the two cluster-cell dispersions with different particle sizes. More gas was produced at the end of 48 h of fermentation and at a faster rate (e.g., shorter $t_{1/2}$ and TR_{max} but higher R_{max}) from the two cluster-cell dispersions than the smaller particle single-cell or cell-fragment dispersions.

There were differences between the dispersions that had been pH-treated/washed *in vitro* and those that had not in terms of total gas ($DMCV_{48}$) and time of maximum rate of gas production (TR_{max}). The cell wall particles that had gone through the pH washing treatment procedure produced significantly less gas than those that had not ($DMCV_{48}$ nontreated > $DMCV_{48}$ treated), although the differences were not as great compared to the two types of particles, and there were insignificant differences in $t_{1/2}$ and R_{max} (Table 2).

Figure 3 shows the CLSM images taken shortly after the addition of inoculum (~20 min) and 12 and 48 h after fermentation for the cluster-cell particles (CWP1) and cell-fragment particles (CWP4). Cell wall particles were still visible at the end of 48 h of fermentation, which indicates that not all of the cell wall matrix had been broken down during the fermentation process. However, it was interesting to observe that the morphology of the particles was similar from 12 h onward for the originally large cluster-cell substrate and the smaller cell-fragment substrate. Image analyses show that, after 12 h of fermentation, the particle sizes of all four substrates were similar, in the range of ~50−100 μm. The fact that the cell cluster structure (CWP1) was almost completely lost and reduced to small cell fragments by 12 h of fermentation suggests that part of the fermentation process leads to weakening of the junctions between cells. The preferential attachment of bacteria within cell clusters (CWP2 non-pH-treated) around junctions between cells at the early stage of fermentation (2 h) was observed by CSLM (Figure 4).

SCFA Profile. The SCFA concentrations produced after 48 h of fermentation are summarized in Table 3 as well as the BCR, final pH, and ammonium concentration. Figure 5 presents the total SCFA profiles of the substrates as a function of the fermentation time. Similar to the gas production results, a significant difference between the substrates was observed from 18 h of *in vitro* fermentation. The total SCFA production was similar between the cluster-cell particles (CWP1-W and CWP2-W) and between single-cell particles (CWP3-W) and cell-fragment particles (CWP4-W). However, the large cluster-cell particles (CWP1 and CWP2) led to the production of more SCFAs than the smaller particles (CWP3 and CWP4). This suggests that large cluster-cell particles were more effective compared to the small particles for the bacteria colonation and production.

For all substrates, the main SCFA produced was acetic acid (61.0−66.0%), followed by propionic acid (17.2−18.5%), butyric acid (9.0−11.7%), valeric acid (2.9−4.1%), isovaleric acid (2.4−4.0%), and isobutyric acid (1.5−3.0%). For the washed substrates, it seems that the fermentation of larger particles (CWP1-W and CWP2-W) led to the production of more acetic and propionic acids compared to the smaller particles (CWP3-W and CWP4-W). This result is consistent with more activity by similar types of bacteria rather than different types of bacteria being involved.

In Table 3, it can be seen that the effect of the treatments (CWP1−CWP4) and pH treatment (washed or control) were highly significant for the total SCFAs produced, the

Table 2. Effect of the Particle Structure on *in Vitro* Fermentation Parameters of the Substrates Expressed by the Cumulative Gas Production after 48 h of Fermentation ($DMCV_{48}$, mL/g of DM), Half Time of Asymptotic Gas Production ($t_{1/2}$, h), Maximal Rate of Gas Production (R_{max}, mL/h), and Time of Maximal Rate of Gas Production (TR_{max}, h)[a]

treatments	$DMCV_{48}$ (mL/g of DM)	$t_{1/2}$ (h)	R_{max} [mL (g of DM)$^{-1}$ h^{-1}]	TR_{max} (h)
		Particle Structure		
CWP1	365.0 a	15.4 a	23.2 a	13.1 a
CWP2	363.8 a	15.6 a	20.8 a	12.5 a
CWP3	260.5 b	24.9 b	8.8 b	15.6 b
CWP4	238.7 b	28.0 c	7.8 b	17.4 b
MSD[b]	37.99	2.67	3.11	2.08
		pH washing pretreatment		
nontreated	319.7 a	20.8 a	15.2 a	14.0 b
washed	294.3 b	21.1 a	15.1 a	15.3 a
MSD	20.10	1.41	1.64	1.10
		Probability		
particle structure (CWP)	<0.0001	<0.0001	<0.0001	<0.0001
pH/washing (W)	0.0153	0.6241	0.9771	0.0267
CWP × W	0.5365	0.7983	0.0447	0.2493

[a]The mean results reported with different letters within the same column indicate significant difference ($p < 0.05$). [b]MSD = minimum significant difference.

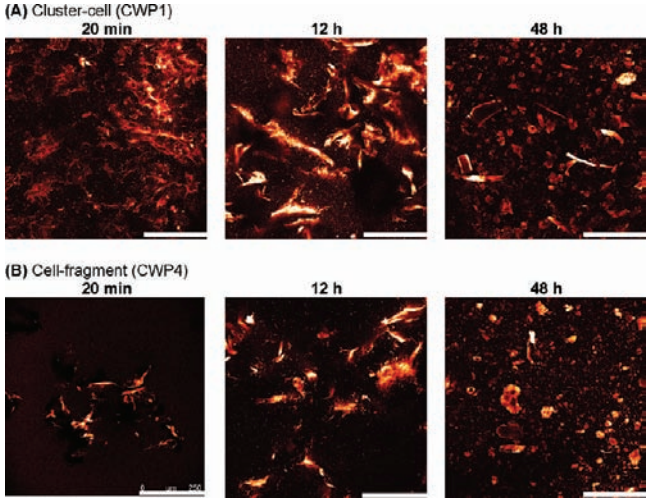

Figure 3. CLSM images showing changes in the particle size and morphology for *in vitro* pH washed cell wall particle dispersions shortly after mixing with colon bacteria (~20 min, time 0) and after 12 and 48 h of fermentation. Scale bar length = 250 μm.

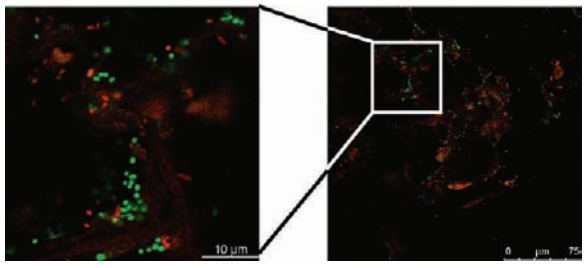

Figure 4. CLSM images showing localized attachment of bacteria in cell clusters (CWP2 non-pH-treated sample) at the early stage of fermentation (2 h). Green- and red-fluorescently stained for live and dead bacteria, respectively. The cell wall background was visualized through autofluorescence.

concentrations of the linear fatty acids produced, as well as the BCR after 48 h of fermentation. The production of branched-chain acids usually results from protein fermentation, whereas straight-chain acids are produced from the fermentation of polysaccharides. pH washing treatment prior to *in vitro* fermentation led to the production of less straight-chain acids and total SCFAs than nonwashed samples. However, in terms of the ratio of the SCFAs produced, the fermentation of the washed substrates was linked with a slightly higher proportion of acetate, propionate, and butyrate compared to the branched-chain acids, leading to a significantly lower BCR than the control. This suggests that the pH washing treatment led to a reduction in N-containing compounds (such as amino acids and soluble proteins) or their reduced availability for fermentation.

DISCUSSION

Fruit and vegetables are a major contributor to the dietary fiber part of food intake. The physiological effect of dietary fibers in terms of health benefits is at least in part linked to their influence on the large bowel microbial diversity and the associated products of fermentation.[5] However, not all fibers exert physiological effects to the same extent. The physio-chemical properties and physical structure of fibers from different sources can have a strong impact on the metabolic effects and systemic physiology of the colon.[15] Particle size, porosity, and surface area characteristics of the fiber can affect the accessibility by bacteria. Studies of fibers from different cereal sources and different sizes of wheat bran fractions (coarse versus fine milling) suggest that smaller particles are fermented more rapidly than larger particles,[29,30] consistent with the specific surface area being a controlling factor. Although a few studies have been conducted to examine the fermentation characteristics of fibers from different types of fruit and vegetable, the relationship between the fiber particle size and their fermentation kinetics has not been investigated previously.

When heating at different temperatures and times is combined with mechanical shearing (blending) at various speeds and times, plant particle dispersions with different particle morphologies were produced. Cell clusters, single cells, or cell wall fragments exhibited different fermentation properties. After an initial phase of comparable properties, the larger cluster-cell particles were fermented more rapidly and to a greater extent than the smaller single-cell or cell-fragment particles, as shown by their cumulative gas product profiles and

Table 3. Effect of the Particle Structure on the Production of SCFAs, BCR, and pH at the End Point (48 h) of Fermentation[a]

treatments	acetic acid (mmol/g of DM)	propionic acid (mmol/g of DM)	butyric acid (mmol/g of DM)	total SCFAs (mmol/g of DM)	BCR	pH	ammonium (mmol/g of DM)
			Particle Structure				
CWP1	10.14 a	2.83 a	1.45 a	15.78 a	0.186 ab	6.69 a	13.67 a
CWP2	8.47 b	2.39 b	1.26 b	13.28 b	0.196 a	6.68 a	12.70 ab
CWP3	7.41 c	2.07 c	1.30 b	11.75 c	0.176 b	6.63 b	10.82 b
CWP4	7.36 c	2.05 c	1.34 ab	11.81 c	0.192 ab	6.68 a	10.86 b
MSD[b]	0.99	0.30	0.14	1.47	0.019	0.041	2.00
			pH washing pretreatment				
nontreated	8.69 a	2.43 a	1.41 a	13.86 a	0.211 a	6.70 a	13.26 a
washed	8.00 b	2.25 b	1.27 b	12.45 b	0.164 b	6.64 b	10.76 b
MSD	0.52	0.16	0.07	0.78	0.010	0.022	1.06
			Probability				
particle structure (CWP)	<0.0001	<0.0001	0.0048	<0.0001	0.0325	0.0043	0.0010
pH washing (W)	0.0120	0.0296	0.0006	0.0010	<0.0001	<0.0001	<0.0001
CWP × W	<0.0001	0.0005	<0.0001	<0.0001	<0.0001	0.0304	0.0549

[a]The mean results reported with different letters within the same column indicate significant difference ($p < 0.05$). [b]MSD = minimum significant difference.

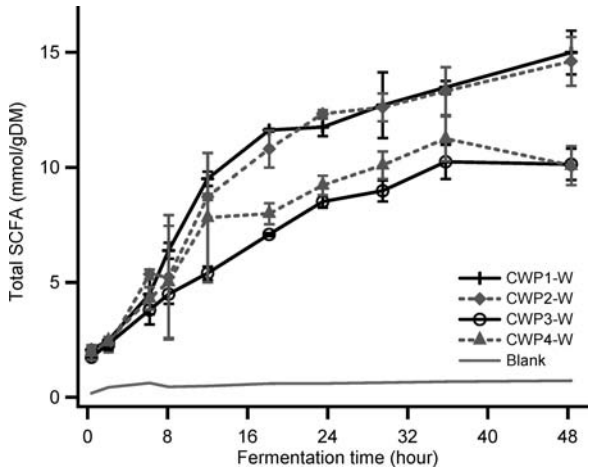

Figure 5. Total SCFAs released as a function of the *in vitro* fermentation time. CWP1, large cluster particles with an average particle size $d_{0.5}$ of 298 μm; CWP2, cluster particles with $d_{0.5}$ of 137 μm; CWP3, single cell particles with $d_{0.5}$ of 75 μm; and CWP4, cell fragment particles with $d_{0.5}$ of 50 μm. W = cell wall dispersions that had gone through pH washing treatment.

production of more SCFAs at the end of 48 h of fermentation. The clear difference between the larger CWP1/CWP2 samples and the smaller CWP3/CWP4 samples was somewhat counterintuitive. Our original hypothesis was that increasing the surface area by breaking the cell wall into smaller particles would lead to an increase in the rate and extent of fermentation. Furthermore, it had previously been reported that increasing the particle size of cereal endosperm cell wall particles or wheat bran fibers decreases their *in vitro* fermentation rate.[29,30]

The fact that there were no systematic differences between fermentation rates during the first 8 h suggests that the amount of readily fermentable material was comparable for all particle sizes, i.e., similar amounts of pectin were accessible by bacteria. This is in contrast to a report that decreased porosity of sugar-beet fiber preparations can result in reduced fermentation over the first 6 h but not subsequently.[39] These qualitative differences between the present results and those for cereal bran and sugar-beet fiber suggest that a different mechanism is operating in carrot cell wall fiber preparations. In contrast to both cereal bran and sugar-beet fibers, the microstructure of processed carrots is relatively open and of low density, which may explain why processing history and particle size had no effect on initial fermentation rates. The difference in fermentation rates from 8 h onward suggests that microbial activity is more favored in the larger (cell cluster) particles compared to the smaller (single cell and fragment) particles. The observation of clustering of bacteria within cell clusters around junctions between cells (Figure 4) suggests that cell junctions within clusters may provide a local microenvironment that is more conducive to bacterial growth than the more exposed surfaces of cell wall fibers that are the predominant site for fermentation in smaller particles. The finding that all substrates had similar particle sizes at the end of *in vitro* fermentation suggests that intercellular adhesion is lost as a result of bacterial action. This susceptibility is analogous to the cell separation induced by heating of most fruit and vegetable tissues (including carrot) and highlights the middle lamella region as a weak point in these tissues.

Further investigations are required to understand the relationships between carrot fiber structure (morphology and particle size) and fermentation. In particular, it would be interesting to determine if the higher amount and faster rate of production of gas and SCFAs from larger particles was due to preferential attachment of bacterial species to cell wall junctions or whether there was a difference in bacterial species as a result of the different microenvironments provided by cell clusters and more isolated cell walls. The effects of processing on the structure/state and properties of the materials are very complex, and further investigations are necessary to improve the understanding of this multivariate relationship.

Although the mechanisms are not yet completely understood, these results can be used for the preparation of functional foods targeting colonic health. To be health-promoting, there needs to be a mixture of fibers that are fermented both rapidly and slowly to provide health effects along the entire large intestine but not too slowly; otherwise, they are excreted before fermentation occurs.[40] According to the results presented in this study, it may be possible to design vegetable-based foods for fiber delivery and promotion of fermentation that act throughout the colon. The potential to modify the amounts and distribution of the end products and the site of

their production in the colon is also likely to be important, because each has implications for human health.

AUTHOR INFORMATION

Corresponding Author

*Fax: +61-3-0731-3250. E-mail: li.day@csiro.au.

Notes

The authors declare no competing financial interest.

ACKNOWLEDGMENTS

The authors thank Helen French and Mi Xu for assisting in sample preparation and particle size measurements.

REFERENCES

(1) He, F. J.; Nowson, C. A.; MacGregor, G. A. Fruit and vegetable consumption and stroke: Meta-analysis of cohort studies. *Lancet* **2006**, *367*, 320−326.

(2) Ness, A. R.; Powles, J. W. Fruit and vegetables, and cardiovascular disease: A review. *Int. J. Epidemiol.* **1997**, *26*, 1−13.

(3) Lim, C. C.; Ferguson, L. R.; Tannock, G. W. Dietary fibres as "prebiotics": Implications for colorectal cancer. *Mol. Nutr. Food Res.* **2005**, *49*, 609−619.

(4) Kristensen, M.; Jensen, M. G. Dietary fibres in the regulation of appetite and food intake. Importance of viscosity. *Appetite* **2011**, *56*, 65−70.

(5) Brownlee, I. A. The physiological roles of dietary fibre. *Food Hydrocolloids* **2011**, *25*, 238−250.

(6) Stephen, A. M.; Cummings, J. H. Mechanism of action of dietary fiber in the human colon. *Nature* **1980**, *284*, 283−284.

(7) Rodriguez, R.; Jimenez, A.; Fernandez-Bolanos, J.; Guillen, R.; Heredia, A. Dietary fibre from vegetable products as source of functional ingredients. *Trends Food Sci. Technol.* **2006**, *17*, 3−15.

(8) Redgwell, R. J.; Fischer, M. Dietary fiber as a versatile food component: An industrial perspective. *Mol. Nutr. Food Res.* **2005**, *49*, 521−535.

(9) Day, L.; Xu, M.; Oiseth, S., K.; Lundin, L.; Hemar, Y. Control of morphological and rheological properties of carrot cell wall particle dispersions through processing. *Food Bioprocess Technol.* **2010**, *3*, 928−934.

(10) Day, L.; Xu, M.; Oiseth, S., K.; Lundin, L.; Hemar, Y. Dynamic rheological properties of plant cell wall particle dispersions. *Colloids Surf., B* **2010**, *81*, 461−467.

(11) Hemar, Y.; Lebreton, S.; Xu, M.; Day, L. Small-deformation rheology investigation of rehydrated cell wall particles−xanthan mixtures. *Food Hydrocolloids* **2011**, *25*, 668−676.

(12) McCann, T. H.; Fabre, F.; Day, L. Microstructure, rheology and storage stability of low-fat yoghurt structured by carrot cell wall particles. *Food Res. Int.* **2011**, *44*, 884−892.

(13) Netzel, M.; Netzel, G.; Zabaras, D.; Lundin, L.; Day, L.; Addepalli, R.; Osborne, S. A.; Seymour, R. Release and absorption of carotenes from processed carrots (*Daucus carota*) using *in vitro* digestion coupled with a Caco-2 cell trans-well culture model. *Food Res. Int.* **2011**, *44*, 868−874.

(14) Eastwood, M. A.; Morris, E. R. Physical properties of dietary fiber that influence physiological function—A model for polymers along the gastrointestinal tract. *Am. J. Clin. Nutr.* **1992**, *55*, 436−442.

(15) Guillon, F.; Champ, M. Structural and physical properties of dietary fibres, and consequences of processing on human physiology. *Food Res. Int.* **2000**, *33*, 233−245.

(16) Ellegard, L.; Andersson, H. Oat bran rapidly increases bile acid excretion and bile acid synthesis: An ileostomy study. *Eur. J. Clin. Nutr.* **2007**, *61*, 938−945.

(17) Jacobs, D. M.; Gaudier, E.; van Duynhoven, J.; Vaughan, E. E. Non-digestible food ingredients, colonic microbiota and the impact on gut health and immunity: A role for metabolomics. *Curr. Drug Metab.* **2009**, *10*, 41−54.

(18) Gibson, G. R.; Probert, H. M.; Van Loo, J.; Rastall, R. A.; Roberfroid, M. B. Dietary modulation of the human colonic microbiota: Updating the concept of prebiotics. *Nutr. Res. Rev.* **2004**, *17*, 259−275.

(19) Li, F.; Hullar, M. A. J.; Schwarz, Y.; Lampe, J. W. Human gut bacterial communities are altered by addition of cruciferous vegetables to a controlled fruit- and vegetable-free diet. *J. Nutr.* **2009**, *139*, 1685−1691.

(20) Nordgaard, I.; Mortensen, P. B. Digestive processes in the human colon. *Nutrition* **1995**, *11*, 37−45.

(21) Hamer, H. M.; Jonkers, D.; Venema, K.; Vanhoutvin, S.; Troost, F. J.; Brummer, R. J. Review article: The role of butyrate on colonic function. *Aliment. Pharmacol. Ther.* **2008**, *27*, 104−119.

(22) Topping, D. L.; Clifton, P. M. Short-chain fatty acids and human colonic function: Roles of resistant starch and nonstarch polysaccharides. *Physiol. Rev.* **2001**, *81*, 1031−1064.

(23) Scheppach, W. Effects of short-chain fatty acids on gut morphology and function. *Gut* **1994**, *35*, S35−S38.

(24) Young, G. P.; Hu, Y.; Le Leu, R. K.; Nyskohus, L. Dietary fibre and colorectal cancer: A model for environment−gene interactions. *Mol. Nutr. Food Res.* **2005**, *49*, 571−584.

(25) Canh, T. T.; Sutton, A. L.; Aarnink, A. J. A.; Verstegen, M. W. A.; Schrama, J. W.; Bakker, G. C. M. Dietary carbohydrates alter the fecal composition and pH and the ammonia emission from slurry of growing pigs. *J. Anim. Sci.* **1998**, *76*, 1887−1895.

(26) Bourquin, L. D.; Titgemeyer, E. C.; Garleb, K. A.; Fahey, G. C. Short-chain fatty acid production and fiber degradation by human colonic bacteria—Effects of substrate and cell-wall fractionation procedures. *J. Nutr.* **1992**, *122*, 1508−1520.

(27) Cummings, J. H.; Beatty, E. R.; Kingman, S. M.; Bingham, S. A.; Englyst, H. N. Digestion and physiological properties of resistant starch in the human large bowel. *Br. J. Nutr.* **1996**, *75*, 733−747.

(28) Rose, D. J.; Patterson, J. A.; Hamaker, B. R. Structural differences among alkali-soluble arabinoxylans from maize (*Zea mays*), rice (*Oryza sativa*), and wheat (*Triticum aestivum*) brans influence human fecal fermentation profiles. *J. Agric. Food Chem.* **2010**, *58*, 493−499.

(29) Stewart, M. L.; Slavin, J. L. Particle size and fraction of wheat bran influence short-chain fatty acid production *in vitro*. *Br. J. Nutr.* **2009**, *102*, 1404−1407.

(30) van Laar, H.; Tamminga, S.; Williams, B. A.; Verstegan, M. W. A. Fermentation of the endosperm cell walls of monocotyledon and dicotyledon plant species by faecal microbes from pigs—The relationship between cell wall characteristics and fermentability. *Anim. Feed Sci. Technol.* **2000**, *88*, 13−30.

(31) Mikkelsen, D.; Gidley, M. J.; Williams, B. A. *In vitro* fermentation of bacterial cellulose composites as model dietary fibers. *J. Agric. Food Chem.* **2011**, *59*, 4025−4032.

(32) Williams, B. A.; Mikkelsen, D.; le Paih, L.; Gidley, M. J. I*n vitro* fermentation kinetics and end-products of cereal arabinoxylans and (1,3;1,4)-β-glucans by porcine faeces. *J. Cereal Sci.* **2011**, *53*, 53−58.

(33) Williams, B. A.; Bosch, M. W.; Boer, H.; Verstegen, M. W. A.; Tamminga, S. An *in vitro* batch culture method to assess potential fermentability of feed ingredients for monogastric diets. *Anim. Feed Sci. Technol.* **2005**, *123*, 445−462.

(34) Groot, J. C. J.; Cone, J. W.; Williams, B. A.; Debersaques, F. M. A.; Lantinga, E. A. Multiphasic analysis of gas production kinetics for in vitro fermentation of ruminant feeds. *Anim. Feed Sci. Technol.* **1996**, *64*, 77−89.

(35) Bauer, E.; Williams, B. A.; Voigt, C.; Mosenthin, R.; Verstegen, M. W. A. Microbial activities of faeces from unweaned and adult pigs, in relation to selected fermentable carbohydrates. *Anim. Sci.* **2001**, *73*, 313−322.

(36) Macfarlane, G. T.; Gibson, G. R.; Beatty, E.; Cummings, J. H. Estimation of short-chain fatty acid production from protein by human intestinal bacteria based on branched-chain fatty acid measurements. *FEMS Microbiol. Ecol.* **1992**, *101*, 81−88.

(37) Baethgen, W. E.; Alley, M. M. A manual colorimetric procedure for measuring ammonium nitrogen in soil and plant kjeldahl digests. *Commun. Soil Sci. Plant Anal.* **1989**, *20*, 961−969.
(38) Sila, D. N.; Smout, C.; Vu, S. T.; Van Loey, A.; Hendrickx, M. Influence of pretreatment conditions on the texture and cell wall components of carrots during thermal processing. *J. Food Sci.* **2005**, *70*, E85−E91.
(39) Guillon, F.; Auffret, A.; Robertson, J. A.; Thibault, J. F.; Barry, J. L. Relationships between physical characteristics of sugar-beet fibre and its fermentability by human faecal flora. *Carbohydr. Polym.* **1998**, *37*, 185−197.
(40) Williams, B. A.; Verstegen, M. W. A.; Tamminga, S. Fermentation in the large intestine of single-stomached animals and its relationship to animal health. *Nutr. Res. Rev.* **2001**, *14*, 207−227.